Well-Ordered Mesoporous Silica and Bioactive Glasses: Promise for Improved Hemostasis

Sara Pourshahrestani

Nahrizul Adib Kadri

Ehsan Zeimaran

Mark R. Towler
Missouri University of Science and Technology, mtowler@mst.edu

Biomaterials Science

REVIEW

Check for updates

Well-ordered mesoporous silica and bioactive glasses: promise for improved hemostasis

Sara Pourshahrestani, [iD] *[a] Nahrizul Adib Kadri, [iD] [a] Ehsan Zeimaran [iD] [b] and Mark R. Towler[c]

Immediate control of uncontrolled bleeding and infection are essential for saving lives in both combat and civilian arenas. Inorganic well-ordered mesoporous silica and bioactive glasses have recently shown great promise for accelerating hemostasis and infection control. However, to date, there has been no comprehensive report assessing their specific mechanism of action in accelerating the hemostasis process and exerting an antibacterial effect. After providing a brief overview of the hemostasis process, this review presents a critical overview of the recently developed inorganic mesoporous silica and bio-active glass-based materials proposed for hemostatic clinical applications and specifically investigates their unique characteristics that render them applicable for hemostatic applications and preventing infec-tions. This article also identifies promising new research directions that should be undertaken to ascertain the effectiveness of these materials for hemostatic applications.

[a]*Department of Biomedical Engineering, Faculty of Engineering, University of Malaya, Kuala Lumpur 50603, Malaysia. E-mail: sara.pourshahrestani@gmail.com, sara.pourshahrestani@um.edu.my; Tel: +60-14-2023115*
[b]*School of Engineering, Monash University, 47500 Bandar Sunway, Selangor, Malaysia*
[c]*Department of Mechanical & Industrial Engineering, Ryerson University, Toronto M5B 2K3, ON, Canada*

1. Introduction

Uncontrolled bleeding and its serious complications remain the leading cause of over 50% of battlefield casualties and 15–25% of trauma deaths in civilian hospitals.[1,2] It is also reported that even when trauma victims survive the initial injury and the hemorrhage is controlled, the large blood loss leaves the victims more vulnerable to acidosis, coagulopathy, infection, and acidosis, and at risk of late morbidity and mor-

Dr Sara Pourshahrestani obtained her MSc in Organic Chemistry (2012) from the University of Isfahan (Iran) and PhD in Biomaterials and Tissue Engineering (2017) from the University of Malaya (Malaysia). Dr Pourshahrestani currently holds a Postdoctoral Fellowship Position at the Department of Biomedical Engineering, University of Malaya. Her current research interests include the development of biomaterials for hemostatic clinical applications and polymer-based biocompo-sites for soft tissue engineering applications.

Sara Pourshahrestani

Dr Nahrizul Adib Kadri is an Associate Professor at the Department of Biomedical Engineering, University of Malaya, Malaysia. He obtained a Master's degree in Biomedical Engineering (MBiomedE) in 2003 from the University of New South Wales, Australia, and his PhD in 2011 from the University of Surrey, United Kingdom in the area of microengineering. His current research interest is in the area of BioMEMS and lab-on-chip, particularly the development of devices for characterisation of cell populations and diagnostic applications. He is also inter-ested in the development of novel biomaterials and sensors for both diagnostic and patient care management purposes.

Nahrizul Adib Kadri

tality because of sepsis and multiple organ failure.[3–5] Despite all of these variable circumstances requiring successful hemostasis and coagulation as well as the significant mortality rates from hemorrhage, little technological progress in hemostatic materials was made over tourniquets or standard gauze dressings until the beginning of the 21st century. Therefore, early and efficient control of the life-threatening hemorrhage by applying hemostatic agents can be of considerable use in saving lives. An ideal hemostatic material is expected to have the following unique properties: (i) the hemostat should possess the capability to form blood clots rapidly; (ii) it should be biocompatible, bactericidal/bacteriostatic, and biodegradable and beneficial for accelerating wound healing; (iii) the stability, cost-effectiveness and safety issues of the hemostat are other key parameters that should be considered.

Hemostats composed of microporous aluminosilicates including zeolites and clays (i.e. kaolin and smectite) are effective hemostatic products recommended by the Committee on Tactical Combat Casualty Care (CoTCCC) that have proven to be efficacious in controlling massive hemorrhage.[6] However, although these animal- and human-free protein products have shown significantly more promise in hemostatic efficiency than other hemostatic products, they have some adverse side effects that cannot be neglected.

For instance, hemostats based on zeolites (i.e. QuikClot™ (QC, Z-Medica, Wallingford, CT) and QuikClot Advanced Clotting Sponge Plus™ (ACS⁺, Z-Medica, Wallingford, Connecticut, USA)) as first generation approved CoTCCC products may not only cause thermal tissue injuries and abnormal foreign-body reactions but also are found to be ineffective in controlling arterial blood flow.[6–8] Second generations of the approved hemostatic products by the CoTCCC including clay hemostats (i.e. QuikClot Combat Gauze™ (QCG, kaolin-coated gauze, Z-Medica, Wallingford, Connecticut, USA) and WoundStat™ (WS, smectite mineral powder, TraumaCure Inc.,

Bethesda, MD, USA)) were also unable to provide immediate hemostasis, leading to larger blood loss.[6] Moreover, the WS as a backup agent to QCG was later removed from the Tactical Combat Casualty Care (TCCC) Guidelines as it led to embolic, thrombotic, and tissue complications in in vivo models.[6] The presence of these adverse side effects, therefore, has stimulated the search for alternative inorganic hemostatic agents.

Recently, mesostructured materials including mesoporous SiO_2, mesoporous bioactive glasses and their composites have opened a new direction in the field of hemostasis due to their highly mesoporous structure. Similar to zeolite- and clay-based hemostats, porous silica-based materials have demonstrated great promise in promoting the coagulation cascade and achieving desirable hemostasis while overcoming the dangerous side-effects of these inorganic hemostats. Herein, we will briefly describe the principles behind the hemostasis process and the preparation of the mesoporous SiO_2 and mesoporous bioactive glasses. Then, we list the different types of porous materials that have been investigated for hemostatic applications thus far. The proposed mechanisms of action by which they accelerate the hemostasis process and control infection will also be highlighted.

2. Mechanism of hemostasis

Hemostasis, or coagulation, is a physiological process that results in the formation of a stable and insoluble hemostatic plug at an injury site while preserving blood flow normally elsewhere in the circulation.[9] The clotting process proceeds in two phases, primary (platelet plug formation) and secondary hemostasis (coagulation cascade). Fig. 1 schematically presents the details of the hemostasis process.

The primary hemostasis phase refers to the formation of a primary platelet plug and starts immediately after vascular

Ehsan Zeimaran

Dr Ehsan Zeimaran obtained his MSc in Polymer Technology from the University of Technology, Malaysia in 2011 and his PhD in Biomaterials and Tissue Engineering from the University of Malaya in 2016. He is currently a Research Fellow in Monash University. His research interest focuses on biopolymers, bioceramics, and more specifically bioactive glasses and biocomposites for biomedical and tissue engineering applications.

Mark R. Towler

Dr Towler is a Professor of Biomedical Engineering at Ryerson University with a cross-appointment in St Michael's Hospital. Prior to this, he was the Inamori Professor of Biomaterials at Alfred University. He has a PhD from Queen Mary College (University of London, UK) and is the inventor of an in vitro diagnostic, Osentia (http://www.osentia.co.uk). He has published over 150 peer reviewed papers, holds five granted patents and has secured over C$23 million of research funding. He has supervised 16 PhD and 16 MASc students and mentored 17 post-doctoral fellows. Towler was recently awarded the James M Flaherty Visiting Professor position for 2018.
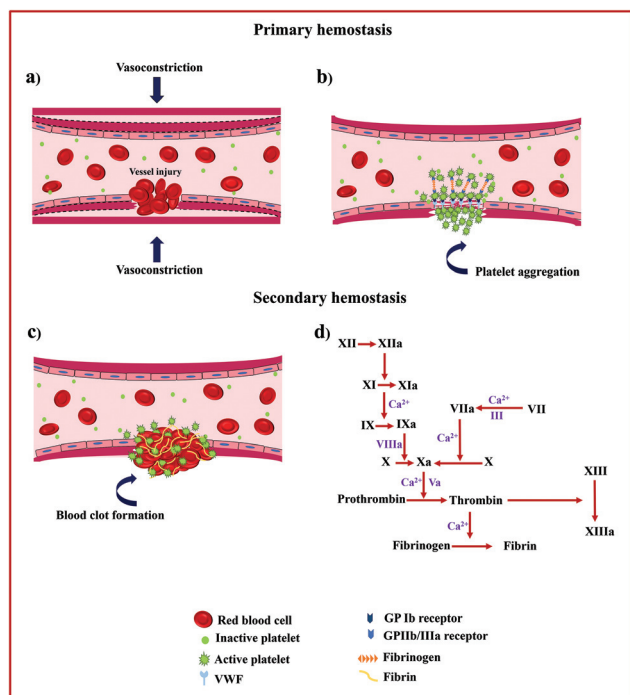
Fig. 1 Schematic diagram of primary and secondary hemostasis. Primary hemostasis: (a) vasoconstriction and (b) primary platelet plug formation. The VWF binding to GP Ib receptors on the platelet surface and platelet binding to fibrinogen *via* platelet surface receptors GPIIb/IIIa lead to platelet aggregation. Secondary hemostasis: (c) a stable and permanent plug trapped within a fibrin network is formed resulting from the activation of (d) the coagulation cascade.

injury and endothelial disruption and involves two processes, namely vasoconstriction and platelet plug formation.[10] Following vasoconstriction that compresses the blood vessels and reduces blood flow, exposed collagen from the damaged blood vessel will encourage platelets to bind to von Willebrand Factor (VWF) on exposed subendothelial collagen *via* glycoprotein Ib (GP Ib) receptors. This receptor–ligand interaction starts the process of platelet activation that leads to cytoskeletal rearrangement, shape change, and release of intracellularly stored granules by multiple signalling pathways. These granules contain substances such as thromboxane A2 (TXA2), adenosine diphosphate (ADP), and serotonin, which not only promote vasoconstriction but also lead to conformational change in platelet surface receptors GPIIb/IIIa inducing binding to fibrinogen and subsequent platelet aggregation.[11]

This phase of hemostasis is temporary, resulting in primary clot formation, which halts bleeding primarily. Secondary hemostasis phase refers to the coagulation cascade consisting of two main pathways, intrinsic and extrinsic coagulation pathways, which produces an insoluble fibrin mesh to strengthen and stabilize the platelet plug. For the intrinsic pathway (contact activation pathway), the negatively charged surface activates factor XII, a plasma protein, upon blood vessel damage, leading to the activation of other coagulation

factors.[12] In contrast, the extrinsic pathway (tissue factor pathway) starts when injury to the blood vessel wall exposes tissue factor (TF) to blood, which in turn leads to the activation of coagulation factor VII (FVII) in the presence of calcium ions (Ca^{2+}).

Both the intrinsic and extrinsic pathways converge into a final common pathway that initiates *via* the activation of factor X, an enzyme that merges with a cofactor, activated factor V (FVa), and Ca^{2+} to form a prothrombinase complex that eventually helps to cleave prothrombin into thrombin.[13] Thrombin is a serine protease responsible for the conversion of soluble fibrinogen into insoluble fibrin and catalyses many other reactions in the blood coagulation cascade. Finally, the fibrin monomers combine to form long fibrin threads that serve to strengthen and stabilize the primary platelet plug and to form actual blood clots by activated factor XIII, a fibrin-stabilizing factor, and Ca^{2+}.[14]

3. Mesoporous SiO_2

The term "mesoporous materials" refers broadly to materials with pore sizes of 2 to 50 nm.[15] Silica-based ordered mesoporous materials (SMMs) (*i.e.* Mobil Composition of Matter No. 41 (MCM-41), Mobil Composition of Matter No. 48 (MCM-48), and Santa Barbara Amorphous (SBA-15)) have recently attracted worldwide attention because of their significant features of good biocompatibility, low cytotoxicity, thermal stability, and tailorable surface charges as well as having larger pore sizes and pore volumes than zeolites.[16–18] The materials were first introduced in the early 1990s.[19] These porous materials are structurally unique, exhibiting disorder on the atomic scale and well-defined order on the mesoscopic-scale (2–50 nm). Two different mechanisms are involved in the formation of SMMs, namely the true-liquid-crystal template (TLCT)[20] and cooperative liquid crystal template (CLCT)[21] mechanisms (Fig. 2). In the TLCT mechanism (Route 1), the structure directing agent (SDA) concentration exceeds the critical micellar concentration (cmc) so that under the prevailing conditions (temperature and pH) and without requiring the existence of inorganic precursors, the surfactant molecules arrange themselves to form liquid-crystalline phase (Fig. 2a).[22] In contrast, in the CLCT mechanism (Route 2), the lyotropic liquid crystalline phase is formed through cooperative self-assembly of the SDA at lower concentration and inorganic precursors, leading to the formation of ordered mesostructures with laminar, hexagonal or cubic arrangements (Fig. 2a).[23] At the final step of both synthetic processes, the template needs to be removed, resulting in the formation of a network of cavities within the silica framework and SMMs are therefore obtained with outstanding properties, such as: (i) regular and tunable meso-pore size (2–50 nm), (ii) high surface area (*ca.* 1000 m^2 g^{-1}), (iii) large pore volumes (*ca.* 1 cm^3 g^{-1}), (iv) homogeneous pore morphology and (v) stable mesoporous structure.[24] Over the past two decades, research studies on the SMMs have demonstrated their suitability for two new appli-
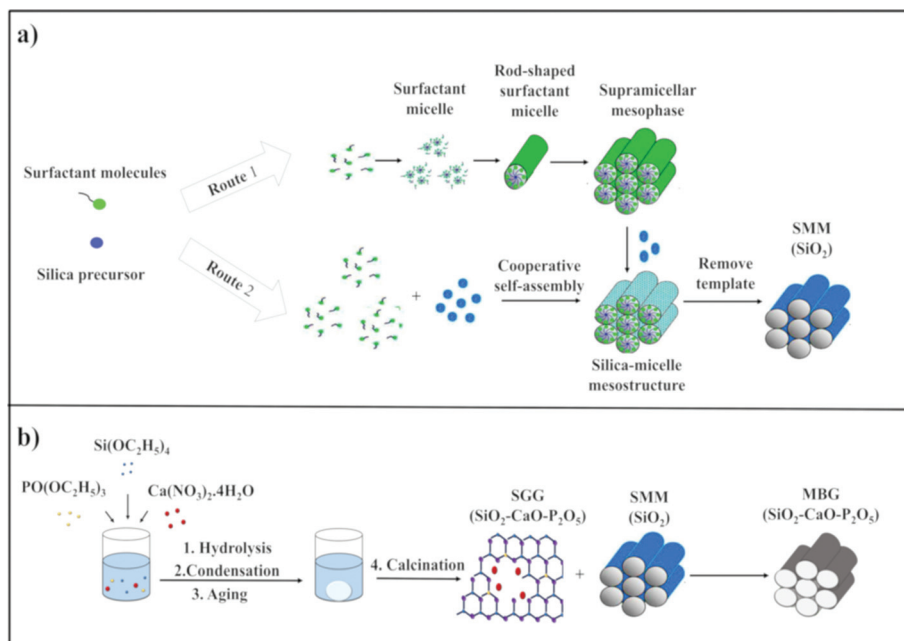
Fig. 2 Schematic representation of the synthesis of (a) SMM *via* TLCT (Route 1) and CLCT (Route 2) and the synthesis of (b) MBG based on the combination of supramolecular chemistry of SMM and sol–gel technology of SGG.

cations, namely drug delivery and bone regeneration applications based on their unique textural properties. The materials were found to have high drug and biologically active molecule loading and releasing abilities.[25–31] Additionally, the *in vitro* bioactivity of three typical SMMs, namely MCM-41, SBA-15 and MCM-48, was investigated and the materials were demonstrated to have the potential to form an apatite-like layer on their surfaces upon immersion in a simulated body fluid (SBF), allowing their use in bone tissue regeneration.[32]

4. Mesoporous bioactive glasses (MBGs)

A new generation of nanostructured bioceramics, referred to as mesoporous bioactive glasses (MBGs) in the 80% SiO_2–15% CaO–5% P_2O_5 system, was first developed by Yan *et al.*[33] in 2004 through a sol–gel route combined with supramolecular chemistry of sol–gel glasses (SGGs) and SMMs, respectively (Fig. 2b).[34] In this strategy for the preparation of MBG, the incorporation of SDAs such as Pluronic P123, F127 and cetyltrimethyl ammonium bromide (CTAB) is vital for acquiring well-ordered structures similar to that for SMMs.[35] Under appropriate synthesis conditions, the mixture reaction system of SGGs and SDAs undergoes an evaporation induced self-assembly (EISA) process. The EISA process starts with a homogeneous solution of SGG precursors (*i.e.* Si, Ca and phosphorus (P) elements) and the surfactant prepared in an ethanol–water solution. After ethanol evaporation that increases the concentration of the system until cmc is reached, self-assembled silica–surfactant micelles with spherical or

cylindrical structures are formed and with further increase of the surfactant concentration, liquid crystalline mesophase is developed by the self-organization of the micelles.[36] Finally, a well-ordered mesoporous structure is obtained after surfactant removal by extraction or calcination methods. It should be mentioned that the MBGs not only share a similar structural and textural properties to the SMMs but also possess a similar amorphous atomic structure in the ternary system SiO_2–CaO–P_2O_5 to that of the SGGs.[24] However, the main difference between MBGs and SGGs can be summarized basically in the mesoscale, which is not presented in the SGGs.[37]

The ordered mesoporous arrangement in the MBGs can produce surface area and pore volume remarkably larger than those obtained in the SGGs.[37,38] These outstanding features have resulted in materials with improved *in vitro* bioactivity and excellent cytocompatibility as compared with conventional SGGs, thus making them attractive for bone tissue engineering applications.[34,35,39–44] Additionally, the excellent surface properties and porosity as well as their high ability for functionalization render such promising candidates local-controlled delivery systems of drugs (antibiotics and/or osteogenic agents) to treat bone pathologies.[24,45–49]

5. Hemostatic potential of mesostructured materials

Recently, SMMs and MBGs in the form of macro and nano particles, microspheres, foams and composite scaffolds have been proved to promote hemostasis due to their blood clot-promoting surfaces, porous structures and their fast plasma absorb-

ability without damaging thermal profile of zeolite-based hemostats. The materials are also found to prevent infections through releasing antibacterial elements from their frameworks. In the following sections, recent advances in SMMs, MBGs and their composite forms for hemostatic applications are discussed and the effect of several factors including their surface chemistry, textural properties (*i.e.* surface area, porosity and pore size) and morphological characteristic (*i.e.* form) that seem to govern their hemostatic functions are also highlighted. The sections below also elucidate the influence of therapeutic ions released from MBGs and SMMs-framework resulting from their dissolution in biological contexts on blood clot formation and microbial function. Fig. 3 depicts the mechanisms of action of the reported therapeutic ions released through SMM and MBG dissolution that are believed to stimulate hemostasis and exert antibacterial effects.

5.1. The surface area, Si/Ca ratio, and morphology of SMMs and MBGs

Among all the parameters governing the hemostatic effects of SMMs and MBGs, high surface area and porosity are important factors that improve the adsorption capacity of the materials. SMMs and MBGs featuring high surface area can promote hemostasis by absorbing a large amount of water from the blood and condensing the clotting factors and platelets. In addition to the available surface area and porosity, the Si : Ca ratio and availability of Ca^{2+} ions are other important parameters that contribute to the hemostatic ability of the materials.[50]

The Ca^{2+} ions, considered clotting factor IV, are critical ions in the clotting cascade which function as a cofactor with other clotting factors and are involved in the activation of both intrinsic and extrinsic pathways.[51] When the ions are released from the porous silica network, they enhance thrombin generation, which not only play a vital role in the initiation of platelet activation and aggregation, but also contribute to the conversion of fibrinogen into stable fibrin clot.[51,52] The water adsorption ability of the mesoporous materials is also improved by the Ca^{2+} ions that reside in the pores. Indeed, the electrostatic attraction between water and Ca^{2+} ions may result in enhanced water adsorption.[53,54] The particle morphology is another important factor affecting the hemostatic function of the SMMs and MBGs. Spherical particles, for example, have been demonstrated to provide more available surface to blood compared to irregular particles and facilitate blood clot formation.[50]

Taking advantage of these features, bioactive glasses with different textural properties and Si : Ca ratios were developed in a study by Ostomel *et al.*[50] and their hemostatic potentials have been identified for the first time. In this study, the hemostatic responses of porous and non-porous bioactive glasses and porous and nonporous spherical bioactive glasses were evaluated using a thromboelastogram (TEG) analyser (a hemostasis analyser that tests the efficacy of blood coagulation through measuring the strength and stability of the formed blood clot) when the Si : Ca ratio was increased. The authors claimed that not only high surface area, porosity, Si : Ca ratio and availability of Ca^{2+} ions are important parameters contributing to the hemostatic performance of glasses but also the shape and particle morphology of the glasses play an important role in decreasing the clotting time.[50] According to their results, on increasing the Si : Ca ratio in the glasses, both the time until clot detection (R) and coagulation rate (α) were decreased and increased, respectively, and porous and spherical bioactive glasses were found to be superior to other materials as they showed faster coagulation. However, in comparison with irregular porous glass, spherical glass resulted in faster clotting for a given similar Si/Ca ratio. Towards a better understanding of the hemostatic effects of bioglasses, the thrombogenicity of the SBA-15 and CaO (model components of bioglass-based hemostat) as well as hydroxylapatite [$Ca10(OH)_2(PO_4)_6$], nonporous SiO_2 glass beads and $CaCO_3$ (models of Si and Ca-containing oxides) was also investigated in this study.[50] With the exception of [$Ca10(OH)_2(PO_4)_6$] that showed an antithrombotic effect and delayed coagulation, all samples demonstrated reduced R. Furthermore, unlike CaO and $CaCO_3$ that resulted in the faster rates of coagulation and stronger clots, both α and maximum clot strength (MA) decreased on increasing the SBA-15 content despite reducing R. On the basis of these results, it was speculated that the presence of Ca^{2+} in both CaO and $CaCO_3$ was likely to contribute to their hemostatic actions.[50] Their study also demonstrated that the glasses possess clotting efficacy comparable to the zeolite-based hemostats (*i.e.* QuikClot ™) but without damaging their thermal profile. Porous and non-porous glasses with lower surface area (up to 400 m^2 g^{-1} or greater) compared with zeolite-based hemostatic agents (up to 600 m^2 g^{-1}) have smaller ΔH hydration (up to 400 J g^{-1} with respect to
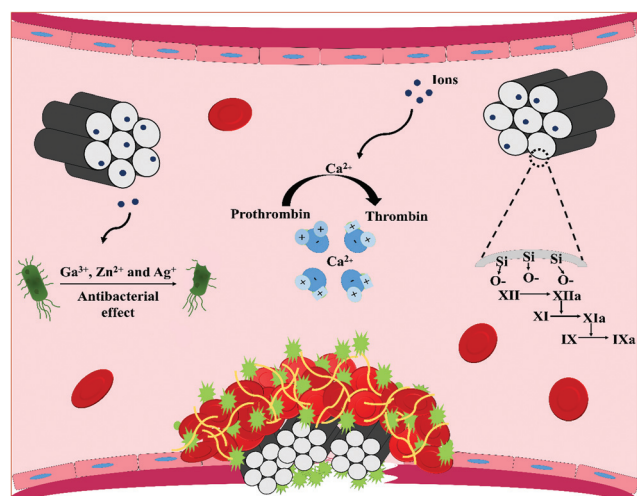
Fig. 3 Schematic summary of the hemostatic function and antibacterial effect of mesostructured materials. They can achieve a rapid hemostasis through (i) their negative surface charge that activates the intrinsic pathway of the coagulation cascade, (ii) acceleration of thrombin formation *via* releasing the Ca^{2+}, and (iii) concentrating the blood components and subsequent clot formation resulting from the interaction of Ca^{2+} residing in their pores with water molecules leading to a high water absorption capacity. They can also exert antibacterial effects through therapeutic elements released from their framework.

700 J g^{-1}), therefore hydrating hemorrhaging blood without heat generation.

A further study by Ostomel et al.[55] also evaluated the hemostatic activity of ordered mesoporous bioactive glass microspheres (MBGMs) with different Si molar contents (60 and 80 mol%) and diameters ranging from 100 nm to 1 μm as compared with non-porous MBGMs using TEG. In the same Si/Ca ratio, MBGMs were found to be more effective in inducing hemostasis with respect to nonporous MBGMs, and on increasing the amount of the samples up to 15 mg, MBGMs not only decreased R from 10.9 min in sheep blood to 2.9 min but also increased α from 50.2° in sheep blood to 72.4° compared to non-porous MBGMs (R = 3.5 min and α = 65°).[55] The study also confirmed a linear relationship between pro-coagulant activity and the ratio of Si/Ca of the glasses, so that increased pro-coagulant activity was observed in MBGM with a higher Si/Ca ratio (80 mol% Si, MBGM-80). This thrombotic effect of the porous materials was ascribable to the presence of negatively charged siliceous oxide (SiOH) on their surface as well as the release of Ca^{2+} ions, which make them capable of concentrating blood components through water absorption of blood.[55] It was argued that even glass with high Si contents can deliver adequate amounts of Ca^{2+} in the wounded area to stimulate an enhanced coagulation response.[55] This study also evaluated the bone-forming ability of the MBGMs and found that in comparison with the glasses with high Si/Ca, glasses with low Si/Ca had a higher ability to nucleate hydroxyapatite (HA) layer when immersed in SBF.[55]

Wu et al.[56] investigated the influence of the surface area, mesoporous structure and Ca^{2+} inclusion on the hemostatic responses of mesoporous silica xerogels (MSX) doped with various amounts of CaO (0, 5 and 10 mol%) by measuring activated partial thromboplastin time (APTT, time to activate the intrinsic pathway) and prothrombin time (PT, time to activate the extrinsic pathway of blood coagulation). The results revealed that both APTT and PT were considerably decreased by m-SXC0 (m-SX without Ca) as compared with non-mesoporous silica xerogels (SX).[56] The in vitro blood coagulation ability of the m-SXC was ascribed to its mesoporous characteristic and higher surface area (489.9 m^2 g^{-1}) compared with that of SX (82.3 m^2 g^{-1}), which resulted in higher water absorption (89% versus 31%), therefore concentrating the blood components and reducing the clotting time. The inclusion of higher Ca^{2+} content in the m-SX framework (m-SXC10) also shortened both APTT (from 8 s in m-SXC0 to 6 s) and PT (from 16 s in m-SXC0 to 10 s), demonstrating an acceleratory effect of Ca^{2+} on the clotting process. The results confirmed that the high surface area, mesostructure and incorporation of Ca^{2+} in the mesoporous silica network are the most important parameters affecting m-SXC's hemostatic properties.[56]

5.2. Influence of the pore size, particle size and shape of mesoporous hemostats

The pore size, particle size and shape of the mesoporous materials have also been observed to be important factors affecting their hemostatic efficacy.

Mesocellular foams (MCFs, SBA-type material) with a range of cell-window sizes (5.9 to 33.1 nm) and cell diameters (10.0 to 52.1 nm) were developed by Baker et al.[57] and the effect of pore window size on blood clot initiation was investigated by TEG measurements in frozen pooled human plasma (PHP). Fig. 4a–c represents scanning electron microscopy (SEM) of MCF particles with a cell window size of 33 nm (MCF-33) particles in low and high resolution alongside high-resolution transmission electron microscopy (TEM). This study demonstrated that the acceleration of clot initiation is associated with window size but not with surface area as increasing the window size from 6 to 33 nm accelerated the blood coagulation so that the clotting time diminished from 9.8 to 6 min. The rate of clot formation was also found to significantly increase when the average window size of the MCFs was >20 nm. Their study also found that immobilizing thrombin in the MCF-33 pores significantly improved its hemostatic ability compared with MCF-33 and QuikClot™ as the clotting times of both PHP and Coumadin plasma were significantly reduced in the presence of MCF-thrombin (Fig. 4d). The higher hemostatic potential of MCF-thrombin was correlated to the synergistic effect of immobilized thrombin and its large protein-accessible surface area, allowing FXII and other contact activation proteins to diffuse into its pores, and activate after adhesion to its negatively charged surfaces, therefore promoting the contact activation of the coagulation cascade.

The potential of MCF with a cell window size of 26 nm (MCF-26) to induce clot formation was also assessed by Li et al.[58] and compared with that of layered clays (i.e. kaolin, bentonite and montmorillonite). The results obtained in this study revealed that all the investigated materials in two different concentrations (3 and 7 mg mL^{-1}) reduced the time to clot formation compared to PHP alone and the clotting activity of MCF-26 at concentrations of 7 mg mL^{-1} was comparable to the clays as there were no statistically significant differences in clotting times of PHP. All MCF-26 and clays reduced the clotting time from 14 min in PHP to ∼6–6.5 min.[58] This result is in good agreement with the findings of a previous study[57] indicating that MCFs with a large window size have the capability to sequester and release pro-coagulant clotting factors at the wounded area. The results additionally showed that MCF-26 is much less cytotoxic toward human cell types (i.e. primary human endothelial and skin cells) with respect to kaolin and other layered clays.[58]

The effects of pore size and particle size on the hemostatic efficiency of mesoporous silica nanoparticles (MSN) were also evaluated by Chen et al.[59] The results of clotting blood test (CBT) displayed that although the variation of pore sizes of MSN from 5 nm to 15 nm significantly shortened the CBT and APTT of rabbit plasma compared to the control (without agent), varying the particle sizes from 60 nm to 220 nm showed a negligible effect on blood coagulation. From the results of TEG, MSNs with up to 10 and 15 nm pore-size were found to have faster blood clot formation, higher clot formation rate and clot strength. MSNs with larger pore size also demonstrated less FXII surplus than other samples due to
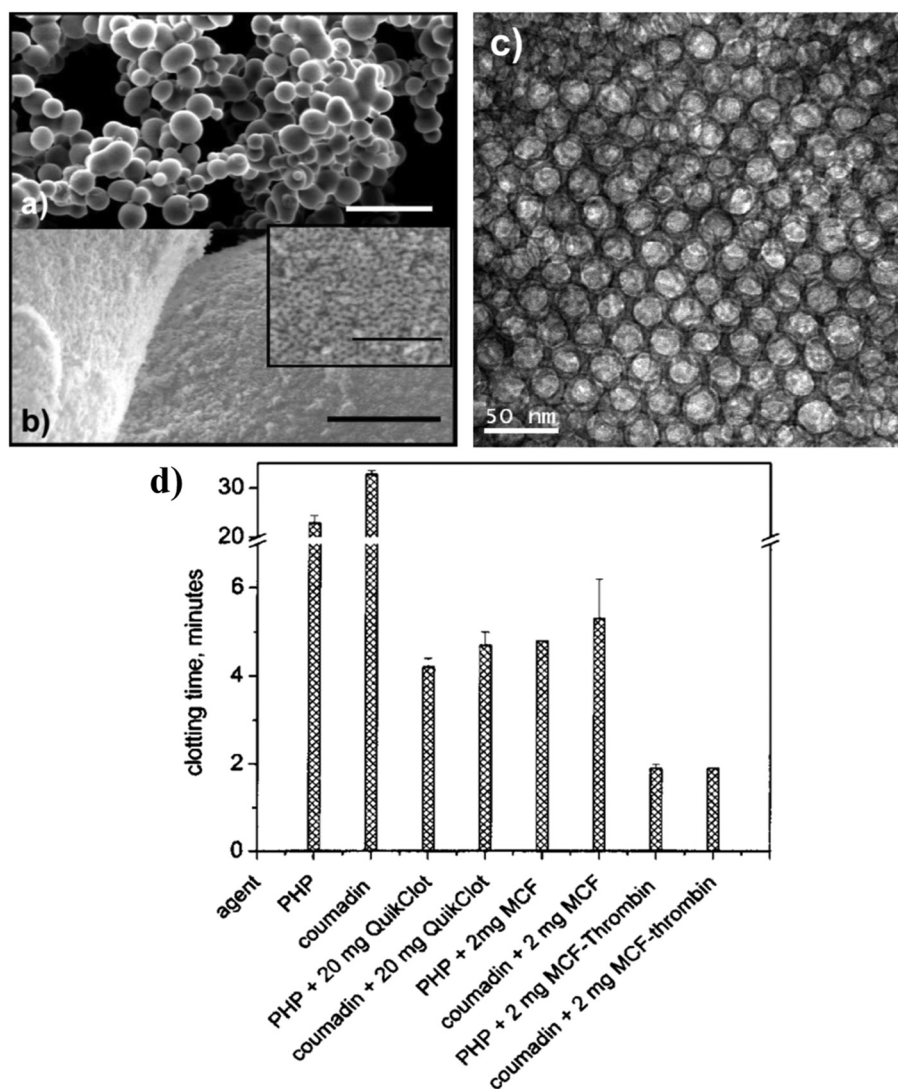
Fig. 4 SEM image of MCF-33 in (a) low and (b) high resolution. (c) High-resolution TEM image of MCF-33. (d) Influence of MCF-33, MCF-thrombin, and QuikClot™ on clotting times of PHP and Coumadin plasma. Reprinted with permission from ref. 57. Copyright 2008, American Chemical Society.

their higher interior surface area allowing more FXII to diffuse into them, convert to FXIIa and diffuse out and accelerating the contact activation pathway. The pore size also impacted the endothelial cell viability so that larger pore size resulted in better biocompatibility. The superior hemostatic efficiency of MSN with a pore size of 15 nm over the standard gauze was also testified *in vivo* since the material achieved rapid hemostasis and reduced mortality to 10.4%, from 100% with the standard gauze in rabbit femoral artery injury.[59]

In addition to pore size and particle size, the form of the mesoporous materials was also shown to affect their hemostatic efficacy. Although porous silica-based materials in particulate form have been found to accelerate hemostasis, similar to zeolite-based hemostats (*i.e.* QuikClot™), the powdery mesoporous materials are reported to have the following shortcomings: (i) the powders cannot be immersed quickly

in blood and can be easily washed away by rapid bleeding from high-flow blood vessels owing to their poor flowability and low density. (ii) They can also form thick callus when the particles are mixed with blood, which makes debridement more difficult.[60] One of the best ways to overcome these problems could be by granulation of the particles.

Hong *et al.*[60] produced different types of mesoporous silica spherical-like granules with diameters ranging from 0.40 to 1.10 mm from mesoporous silica (MPS) particles, polyurethane (PU), sodium pyrophosphate and clay through dry-mixing and wet-granulation methods and evaluated their hemostatic properties in both *in vitro* and *in vivo* with respect to MPS and a MPS mixture (mixture of MPS particles, sodium pyrophosphate and clay). The study found that granulation of the MPS particles can significantly improve their procoagulant activity so that MPS granules (G40 (MPS mixture without PU) and G44

(MPS mixture with PU)) could remarkably decrease the coagulation time and G40 was found to be a more effective hemostatic product, as it significantly reduced the time to hemostasis from 150 s for MPS to 30 s.[60] The authors also evaluated the hemostatic performance of MPS granules *in vivo* in ear and liver injuries in a rabbit model as compared to MPS and MPS was found to be less effective than MPS granules in stopping bleeding. The high hemostatic efficacy of MPS granules was attributed to their higher water absorption capability at the early stage (130%) leading to rapid concentration of blood components and consequently reducing the bleeding time in the wounded area. Additionally, while MPS particles were washed away from injured sites and the wounds were still bleeding, G40 with good flowability could effectively stop bleeding and seal the bleeding vessels. The granule shape of the MPS was also found to play an important role in achieving rapid hemostasis as it provides much greater contact areas when exposed to blood.[60]

5.3. Effect of therapeutic antibacterial element doping on wound infection control

Preventing the spread of infections in the wounded area is another key component of healthcare since wound infections can delay or impair healing and cause life threatening complications.[61,62] Although mesoporous-based hemostats demonstrated promising applicability in the context of hemostasis, they lack antibacterial properties which may limit their applications in the treatment of bleeding, especially the bleeding complicated by infections. The ideal hemostatic agents used for hemostatic applications must promote blood coagulation cascade together with additional features including antimicrobial effects. One of the promising approaches to endow the materials with antibacterial properties is incorporation of therapeutic elements into their frameworks so that the materials acquire antibacterial activities.

Of those available dopants, silver (Ag^+) species have attracted attention due to their antimicrobial activities towards both Gram-negative and Gram-positive microorganisms as well as antibiotic-resistant bacteria.[63–66] The antibacterial action of the ions is linked with three well-defined mechanisms: (i) leading to inactivation of bacteria proteins and enzymes through the reaction with their thiol (sulfhydryl) group, (ii) disrupting membrane permeability and leading to cell lysis and death, and (iii) inhibiting the pathogen's ability to replicate by binding to the bacteria's DNA and RNA.[67–71] Thus, these fascinating characteristics of Ag^+ persuade scientists to incorporate it into the mesoporous-based hemostats. For example, to improve the hemostatic and antibacterial activities of mesoporous silica spheres (MSS), Dai *et al.*[72] first produced calcium-doped MSS (CaMSS) and then loaded it with Ag^+ ions (AgCaMSS) through the exchange method. The authors also prepared AgCaMSS granules with diameters of 600 mm to 1.2 mm *via* the extrusion–spheronization technique. The results from *in vitro* testing showed that inclusion of Ca^{2+} and Ag^+ in the MSS framework increased its clotting activity and led to a remarkable decrease in APTT from 100% in the nega-

tive control (blood-free sample) to ~60%. The presence of Ag^+ was also found to exert a potent antibacterial effect against *Escherichia coli* (*E. coli*) (bacterial reduction of >5.5 log 10) and *Staphylococcus aureus* (*S. aureus*) (bacterial reduction of >4 log 10) as a significant increase in bacterial survival was observed in the CaMSS group.[72] The *in vivo* study also indicated that the time to hemostasis was substantially reduced from 161.2 s in the control group to 9.2 s and 10.6 s in the AgCaMSS group in the form of powders and granules, respectively. The mortality rates for the femoral artery and liver injuries were also decreased in the AgCaMSS powder group (28.6% and 12.5%, respectively) and the granule group (11.1% and 20%, respectively) (Fig. 5) with respect to the positive control group (100%, standard gauze). The higher mortality rate of rabbits treated with powdery AgCaMSS in the artery injury model was correlated to its powder form, which may be easily flushed away by severely bleeding the wounds before they can coagulate blood. These results were in good agreement with those reported by Hong *et al.*,[60] who claimed that powdery MPS can be washed away from the bleeding site, resulting in more bleeding. The study also evaluated the exothermic effects of AgCaMSS in the femoral artery injury model and no remarkable rise in wound temperature (about 4.5 °C) was observed.[72]

In another study, Hu *et al.*[73] evaluated the antimicrobial and hemostatic properties of nanoporous bioactive glass (n-BGS) containing different concentrations of Ag_2O ranging from 0.01 to 0.04 wt% with respect to non-porous bioactive glass (BGS). The results obtained revealed that the incorporation of 0.02 wt% Ag_2O in the n-BGS framework exhibits greater antibacterial activity against *E. coli* than other concentrations with an antibacterial rate of 99% after 12 h incubation. The glass containing 0.02 wt% Ag_2O was found to
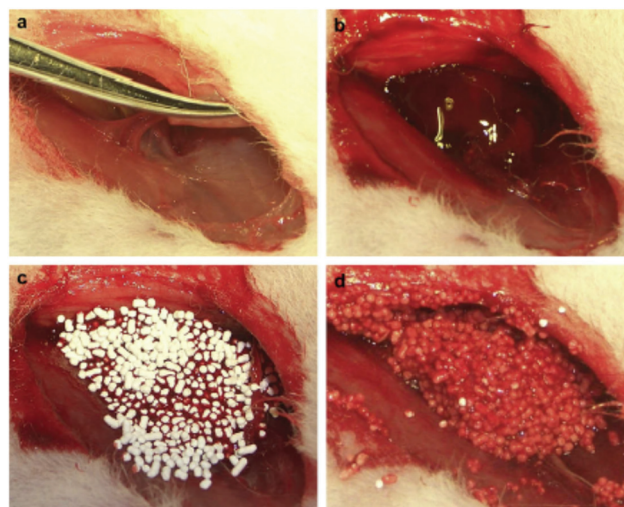

Fig. 5 Stopping bleeding in the rabbit femoral artery injury model. (a) Producing femoral artery injury leading to blood loss. (b) Unopposed hemorrhage at the injured site. (c) Pouring granular AgCaMSS into the wound cavity. (d) The granular AgCaMSS provided rapid and complete hemostasis after compression on the wound. Reproduced with permission from ref. 72. Copyright 2009, Elsevier.

accelerate hemostasis both *in vitro* and *in vivo*. Based on the APTT and PT results, a significant decrease in clotting time was observed in the n-BGS group compared with both BGS and control groups (blood free samples). According to the authors, the higher hemostatic ability of n-BGS was associated with its higher specific surface area (467 m^2 g^{-1}) than that of BGS (91 m^2 g^{-1}). This characteristic makes the n-BGS able to stimulate the blood clot formation through the absorption of a large quantity of water, subsequently facilitating clotting. These results were further confirmed *in vivo*, where the application of the n-BGS to femoral artery and vein injuries of male New Zealand white rabbits reduced the time to hemostasis to 27 s from 86 s and 193 s in BGS and control groups, respectively.[73]

Another well-known antibacterial ion that has been shown to exert antibacterial and antibiofilm properties is gallium (Ga^{3+}), which has an ionic radius similar to that of Fe^{3+} (an important species in the pathogenesis of infections)[74] and can function as a Trojan horse as is indistinguishable from Fe^{3+} for many biological systems.[75] Therefore, Ga^{3+} as a functional analogue of Fe^{3+} was found to be an efficient antibacterial element.

More recently, our group investigated the effect of inclusion of different concentrations of Ga$_2$O$_3$ (1, 2 & 3 mol%) on hemostatic and antibacterial functions of the MBG and found that these functions were considerably affected by the proportion of Ga$_2$O$_3$.[76] Our results demonstrated that the 1 mol% Ga$_2$O$_3$ substituted MBG (1% Ga-MBG) with higher textural properties (*i.e.* surface area = 509 m^2 g^{-1}, pore size = 6.34 nm and pore volume = 0.78 cm^3 g^{-1}), water absorption and Ca^{2+} release rate provided the highest hemostatic performance characteristics compared with MBG and other substituted MBGs (2% Ga-MBG and 3% Ga-MBG). The results obtained on Ga-MBGs confirmed that not only APTT was more reduced in the presence of 1% Ga-MBG compared to other glasses and the control but also platelet adhesion and activation (number of adherent platelets: 1.2 × 10^{12} in MBG *versus* 1.6 × 10^{12} in 1% Ga-MBG after 60 min incubation) as well as thrombus formation (180% in MBG *versus* 230% in 1% Ga-MBG after 60 min incubation) (Fig. 6) were significantly increased in the presence of the glass. It could be also observed that the antibacterial rate of Ga$_2$O$_3$-MBGs against both *E. coli* and *S. aureus* was dependent on the Ga$_2$O$_3$ content so that increasing the Ga amounts up to 3 mol% endowed the MBG with the highest anti-bacterial capacity against *E. coli* (~72%) and *S. aureus* (~99%) with respect to other glasses.

Our recent comparative study further demonstrated that the antibacterial 1% Ga-MBG accelerate hemostasis *in vitro* with greater efficacy with respect to two commercially available hemostats, Celox™ (CX) and ACS$^+$, as it could significantly enhance the activation of the intrinsic pathway, thrombus formation (564% *versus* 245 and 52%, respectively, after 60 min incubation) and thrombin generation (27.22 (ng mL^{-1}) *versus* 13.46 and 8.95 (ng mL^{-1}), respectively, after 60 min incubation).[77] Moreover, larger platelet aggregates and more extensive platelet pseudopodia were observed on the 1% Ga-MBG compared to CX and ACS$^+$, confirming its higher hemostatic

efficacy. The superior thrombogenic effect of 1% Ga-MBG over CX and ACS$^+$ was ascribed to its higher textural properties, allowing it to speedily absorb large amounts of water from the blood, concentrating blood plasma components, and releasing Ca^{2+} ions required for contact activation and therefore promoting hemostasis. Table 1 provides a list of studies evaluating the hemostatic function of SMMs and MBGs.

6. SMMs and MBGs/polysaccharides hemostats

Recently, composites based on the mesoporous materials open up a new avenue for designing desirable materials for hemostatic applications. More recently, the combination of mesoporous materials with organic moieties, which individually have hemostatic effects and work independently of the physiological clotting mechanisms, has been revealed to be another promising strategy that not only can result in the fabrication of efficient composite hemostats with an extraordinary ability to stanch bleeding, but also will eliminate and/or minimize the adverse effects associated with using the mesoporous materials alone. Among various organic compounds, pure polysaccharides have been proved to be efficient in expediting hemostasis.[79]

Chitosan as a natural polysaccharide has been found to be a good candidate to achieve hemostasis independent of the natural coagulation cascade, causes the material to be used as a desirable hemostatic agent and/or as a hemostatic coating layer on the surfaces of medical devices (*i.e.* needle) in the past few decades.[80–83] Chitosan's antihemorrhagic mode of action is thought to be due to electrostatic interaction between the negatively charged cell membrane of erythrocytes and its positively charge surface.[84,85] In comparison with RBCs that are negatively charged due to locating negatively-charged neuraminic acid residues on their surfaces, chitosan is positively charged owing to the presence of some functional groups on its structure such as protonated amino groups in the deacetylated repeat unit. Chitosan not only can induce the adhesion of RBCs on its surface through this ionic interaction, but also can facilitate the blood coagulation cascade through neutralization of the negative charge surface on the RBC surface, leading to their irreversible deformation.[86] Surprisingly, chitosan also seems to be effective in the wound healing process through the activation of macrophages and stimulation of cell proliferation.[87] Therefore, chitosan could be an outstanding candidate for hybrid mesoporous material production.

In a study by Dai *et al.*,[88] a series of CSSX beads composed of mesoporous silica xerogel (MSX) cores and macroporous chitosan layers (CS) were produced *via* the sol–gel process and the polyethylene glycol (PEG) molecular imprinting method. The results indicated that all CSSX beads diminished APTT compared with the negative control (blood without CSSX beads), while there was no effect on the PT of CSSX beads.[88] The underlying causes of shortened APTT and activation of the intrinsic pathway were correlated to the negatively charged surface of MSX and the chitosan coating layer was found to
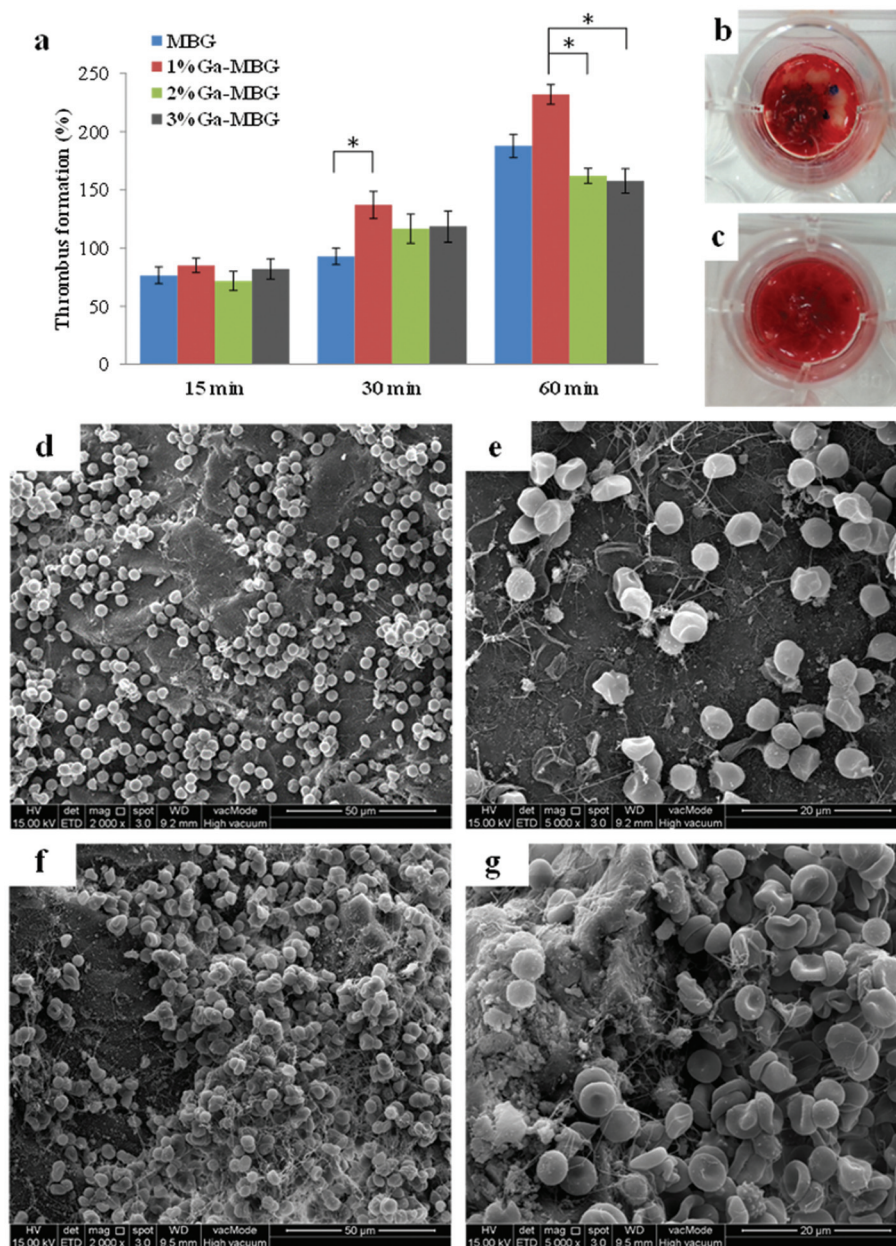
Fig. 6 Thrombus formation on Ga-MBGs. (a) Quantitative analysis of thrombus formation on the glass surfaces after incubation for 15, 30 and 60 min. Photographs of the blood clot formed on the surfaces of (b) MBG and (c) 1% Ga-MBG. Low and high resolution FESEM micrographs of red blood cell (RBC) aggregation and adhesion on (d, e) MBG, and (f, g) 1% Ga-MBG after 30 min of incubation. A large number of RBCs were trapped within a fibrin protein mesh and formed a plug onto the 1% Ga-MBG surface.[76] Reproduced by permission of the Royal Society of Chemistry.

have no substantially effect on APTT. The *in vitro* evaluation of thrombogenic activity also revealed that the amount of blood clot adhered on the surface of CSSX-25 (containing 2% chitosan and 5% PEG) was much higher than that of pure MSX and the control (standard gauze). The superior performance of CSSX-25 was attributed to the interaction of RBCs with CS through their negatively and positively charged surfaces, respectively, leading to the adhesion of more RBCs on CSSX beads. The presence of large and deep pores in the surface of

CSSX-25 also provided additional accessible sites for trapping the blood components. The *in vivo* experimental rabbit model of severe arterial bleeding was also used to test the anti-hemorrhagic effect of CSSX beads (Fig. 7). The rate of survival was 100% in the CSSX bead group while there were no survivors in the control group. A significant improvement in achieving hemostasis and reduction in blood loss was also observed with the application of CSSX-25 beads compared with CSSX-0 (pure MSX).[88]

Table 1 Studies relating to SMM- and MBG-based hemostats

Ref.	Different compositions of SMMs, MBGs and other treatment groups	Textural properties (*i.e.* surface area, pore size and pore volume)			TEG parameters (*i.e.* R (min), α (°) and MA (dyn cm^{-2}))		APTT and PT and/or whole blood clotting time		*In vivo* model	Remarks
		Surface area (m^2 g^{-1})	Pore size (nm)	Pore volume (cm^3 g^{-1})			APTT (s)	PT(s)		
SMM-based hemostats										
56	SX (100% SiO$_2$)	82.3	1.6	—	—		−13	−19	—	- Introducing SX with a mesoporous structure shortened both APTT and PT
	m-SXC0 (100% SiO$_2$)	489.9	3.6				−8	−16		
	m-SXC5 (95% SiO$_2$–5% CaO)	466.5	3.7				−7	−11		- Incorporation of higher CaO content in the m-SXC0 framework resulted in much shorter APTT and PT
	m-SXC10 (90% SiO$_2$–10% CaO)	438.1	3.5				−6	−10		
	Control						−20	−24		
57					R (min)	α (°)	—		—	Increasing the window size from 6 to 33 nm not only decreased the average time to blood clot initiation but also, significantly increased clot strength
	MCF-6 (SiO$_2$)	679	10.0	0.95	−9.8	−42				
	MCF-11 (SiO$_2$)	739	24.5	1.53	−9.6	−43				
	MCF-20 (SiO$_2$)	375	42.7	1.4	−7.2	−41				
	MCF-26 (SiO$_2$)	364	41.9	2.3	−6.8	−61				
	MCF-33 (SiO$_2$)	294	52.1	2.4	−6	−61				
58					At a concentration of 3 mg: R (min)		—		—	Although, at concentrations of 3 mg mL^{-1}, MCF-26 significantly increased the time until clot formation with respect to the layered clays, there was no significant differences between all the samples at 7 mg mL^{-1}
	MCF-26 (SiO$_2$)	—			− 8.4					
	Kaolin				−6.1					
	Bentonite				−6					
	Montmorillonite				−5.9					
					At a concentration of 7 mg:					
	MCF-26 (SiO$_2$)				−6.2					
	Kaolin				−5.8					
	Bentonite				−6.2					
	Montmorillonite				−6					
	PHP				−14.1					
		Surface area (m^2 g^{-1})	Pore size (nm)	Pore volume (cm^3 g^{-1})	R (min)	α (°)	MA (dyn cm^{-2})	APTT (s)	PT (s)		
59	MSN5 + 60 (SiO$_2$)	303	17.2	0.897	2.1	62.0	69.3	−18	−8.4	Femoral artery injury in a rabbit	- While, PT of all MSN groups remained almost unchanged indicating their inability to accelerate the extrinsic coagulation pathway, APTT was significantly shortened in the presence of all the MSN groups with respect to the control. However, there was no significant difference among the MSNs in shortening APTT

Table 1 *(Contd.)*

	Surface area (m² g⁻¹)	Pore size (nm)	Pore volume (cm³ g⁻¹)	R (min)	α (°)	MA (dyn cm⁻²)	APTT (s)	PT (s)	
MSN10 + 60 (SiO₂)	196	47.8	0.974	1.2	63.6	78.5	−17.6	−8.5	- MSN15 + 60 was superior over the standard gauze at achieving hemostasis and reducing blood loss
MSN15 + 60 (SiO₂)	426	61.6	1.446	1.4	71.4	89.7	−17	−8.3	
MSN5 + 100 (SiO₂)	277	10.4	0.721	2.4	61.1	68.7	−17.8	−8.3	
MSN5 + 150 (SiO₂)	390	15.3	0.823	2.8	62.3	67.5	−18.2	−8.4	
MSN5 + 220 (SiO₂)	625	14.5	0.847	3.5	54.9	62.8	−18	−8.6	
Control				9.3	47.0	49.7	−19.6	−8.4	
							Whole blood clotting time (s)		
MSN5 + 60 (SiO₂)									
MSN10 + 60 (SiO₂)							−134		
MSN15 + 60 (SiO₂)							−120		
							−110		
MSN5 + 100 (SiO₂)							−134		
MSN5 + 150 (SiO₂)							−134		
MSN5 + 220 (SiO₂)							−140		
Control							−190		
							Whole blood clotting time (s)		
60 MPS : SiO₂	—			—			−140	The rabbit ear and liver injury model	While MPS particles drifted away from the incision site in both ear and liver injuries and resulted in more bleeding, G40 achieved hemostasis with greater efficacy and successfully sealed the bleeding vessels
MPS mixture: (MPS + clay + sodium pyrophosphate)							−160		
G40: Granules from MPS mixture containing PU							−20		
G44: Granules from MPS mixture without PU							−80		
Control							−390		

MBG-based hemostats

	Si : Ca ratio	Surface area (m² g⁻¹)	At a concentration of 20 mg:					
			R (min)	α (°)	MA (dyn cm⁻²)			
50 BG60	0.37622	339	4.1	69.4	69.8	—	—	On increasing Si : Ca ratio, porous and spherical bioactive glass was superior to other glasses tested in this study as resulted in faster coagulation
BG60NP	0.26298	123	4	58.2	80.6			
BG60SPNP	1.45929	—	3	75.3	69.8			
BG60SP	1.60423	—	4.5	71.7	69.5			
BG80NP	1.2071	197	3.8	71.7	74.8			
BG80	1.75583	420	3.6	71.1	78.2			
BG80SPNP	2.46971	—	2.7	76.1	72.7			
BG80SP	5.94941	386	2.9	79.8	69.4			

Published on 05 October 2018. Downloaded on 3/1/2023 4:53:45 PM.

This journal is © The Royal Society of Chemistry 2019

Biomater. Sci., 2019, **7**, 31–50 | 43

Biomaterials Science

Review

Table 1 *(Contd.)*

MBG-based hemostats

		Si : Ca ratio	Surface area ($m^2\ g^{-1}$)	At a concentration of 20 mg:						
				R (min)	α (°)	MA (dyn cm^{-2})				
55		$SiO_2 : CaO : P_2O_5$		At a concentration of 5 mg:			—		—	- Porous MBGMs demonstrated better coagulation properties than nonporous MBGMs
	MBGM-80	80 : 16 : 4	—	3.6	68.1	77.1				
	MBGM-60	60 : 36 : 4		4.3	72.4	74.3				
	MBGM-80 NP	80 : 16 : 4		4.8	59.3	69.4				
	MBGM-60 NP	60 : 36 : 4		5.2	62.4	74				
				At a concentration of 10 mg:						
	MBGM-80	80 : 16 : 4		3.6	70.6	72.6				- The glass with higher Si/Ca (MBGM-80) showed the greatest hemostatic activity
	MBGM-60	60 : 36 : 4		4.2	74.1	70.2				
	MBGM-80 NP	80 : 16 : 4		4.4	62.9	69.9				
	MBGM-60 NP	60 : 36 : 4		4.2	74.1	70.2				
				At a concentration of 15 mg:						
	MBGM-80	80 : 16 : 4		2.9	72.4	73.4				
	MBGM-60	60 : 36 : 4		3.9	58.6	74				
	MBGM-80 NP	80 : 16 : 4		3.5	65	69				
	MBGM-60 NP	60 : 36 : 4		3.3	69.5	68.5				
	Sheep blood alone			10.9	50.2	58				
				At a concentration of 15 mg:			At a concentration of 2 mg:			
							APTT (%)	PT (%)		
72	AgCaMSS (SiO_2–CaO–P_2O_5, Ag_2O)		—	2.9	71.5	66.0	−60	−106	Rabbit's femoral artery and liver injuries model	- AgCaMSS and CaMSS were more effective than MSS and the control as they significantly decreased and increased R and both α and MA, respectively
	CaMSS (SiO_2–CaO)			2.6	73.0	67.5	—	—		- Although APTT was more shortened in the presence of AgCaMSS compared to MSS, PT remained unchanged
	MSS (SiO_2)			3.6	59.5	58.5	−62	−102		
	Control			9.1	46.0	49.0	100	100		
							At a concentration of 5 mg:			- The application of AgCaMSS in both GA and PA groups led to significantly decreased mortality rate in the rabbit model of femoral artery and liver injuries
	AgCaMSS						56	99		
	CaMSS						—	—		
	MSS						66	96		
	Control						100	100		

		Surface area (m² g⁻¹)	Pore size (nm)		APTT (s)	PT (s)		
78	BGS (SiO₂-CaO P₂O₅, 0.02 wt% Ag₂O)	91	—	—	−40	−130	Rabbit femoral artery and vein injuries model	- The n-BGS was found to have significantly shorter APTT and PT values compared to BGS and control
	n-BGS (SiO₂-CaO-P₂O₅, 0.02 wt% Ag₂O)	476	6		−20	−60		- The n-BGS possessing higher surface area afforded by the mesoporous structure showed higher hemostatic performance than the BGS and control *in vivo* model
	Control				−70	−170		

						At a concentration of 5 mg:			
		SiO₂ : CaO : P₂O₅ : Ga₂O₃	Surface area (m² g⁻¹)	Pore size (nm)	Pore volume (cm³ g⁻¹)	APTT (%)	PT (%)		
76	MBG	80 : 15 : 5	415	5.75	0.55	−42	−104	—	- While all glasses, particularly 1% Ga-MBG, could significantly decrease APTT compared to control, confirming the ability of glass to activation of intrinsic pathway, they did not have ability to decrease PT
	1% Ga-MBG	79 : 15 : 5 : 1	509	6.34	0.78	−36	−108		- No dose-dependent trend was observed in APTT values
	2% Ga-MBG	78 : 15 : 5 : 2	396	5.74	0.54	−38	−100		
	3% Ga-MBG	77 : 15 : 5 : 3	340	6.65	0.52	−46	−108		
						At a concentration of 10 mg:			
	MBG	80 : 15 : 5				−37	−120		
	1% Ga-MBG	79 : 15 : 5 : 1				−33	−124		
	2% Ga-MBG	78 : 15 : 5 : 2				−39	−112		
	3% Ga-MBG	77 : 15 : 5 : 3				−45	−113		
	Control					100	100		

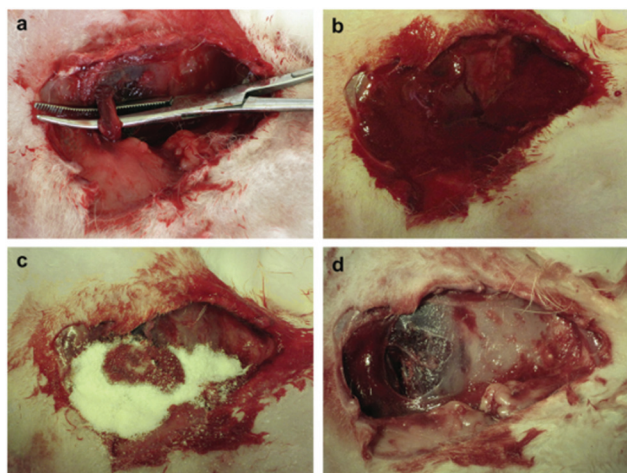|						At a concentration of 5 mg:			
		Surface area (m² g⁻¹)	Pore size (nm)	Pore volume (cm³ g⁻¹)		APTT (s)	PT (s)		
77	1% Ga-MBG	597	5.3	0.77	—	28.87	12.31	—	The 1% Ga-MBG was found more efficient hemostat as resulted in faster blood coagulation
	ACS⁺	561	8.5	0.124		34.71	11.96		
	CX	1.00	6.2	0.003		149.66	14.14		
						At a concentration of 10 mg:			
	1% Ga-MBG					19.55	13.5		
	ACS⁺					26.81	12.7		
	CX					600	74		
	Negative control					44.26	12.21		

Fig. 7 (a) Creation of injury in the rabbit femoral artery. (b) Severe bleeding instantly after injury creation. (c) Pouring CSSX-25 beads into the injury site after suctioning the blood. (d) Irrigating the CSSX-25 beads from the injured site at 180 min. Hemostasis was achieved and no evidence of necrosis was observed at the surrounding tissues. Reproduced with permission from ref. 88. Copyright 2010, Elsevier.

Further studies also compared the hemostatic performance of the porous materials/polysaccharide composites with the pure polysaccharides and it was found that the pure polysaccharide-based hemostats are less efficient at accelerating blood clotting than the composites. A series of chitosan-based composite scaffolds containing different concentrations (10, 30, and 50 wt%) of 1% Ga-MBG (Ga-MBG/CHT) were recently developed by our group using a freeze-drying technique.[89] In this study, we assessed the effect of Ga-MBG inclusion on the hemostatic response of the CHT scaffold in comparison with Celox Rapid gauze (CXR, chitosan-coated gauze).[90] We found that Ga-MBG/CHT composite scaffolds with porous structure and porosity of >79% were capable of absorbing a large amount of water and blood into their pores. The incorporation of 50 wt% of Ga-MBG into the CHT (50% Ga-MBG/CHT) resulted in more desirable hemostasis than other scaffolds and CXR. The 50% Ga-MBG/CHT could trap a large number of RBCs and form a stable blood clot on its surface and pores so that less hemoglobin was released from coagulated RBCs (Fig. 8). More platelets were also adhered and activated on its surface and pores compared with pure CHT and CXR, resulting in a larger hemostatic plug. The results also revealed that incorporation of 50% Ga-MBG into CHT led to higher antibacterial efficacy and biocompatibility than that of CHT and CXR.

Microporous starch (MS) is another polysaccharide-based hemostat that is found to have high hemostatic efficacy owing to its huge surface area, high porosity, and extraordinary water absorption. It can form a hemostatic clot though absorbing the fluid from the blood and therefore increasing the platelet concentration at the site of bleeding. Although MS was found to be effective in controlling low bleeding flow,[91] its main limitation is a lack of sufficient hemostatic capacity in severe and heavy bleeding.[92,93] To improve the hemostatic efficacy of
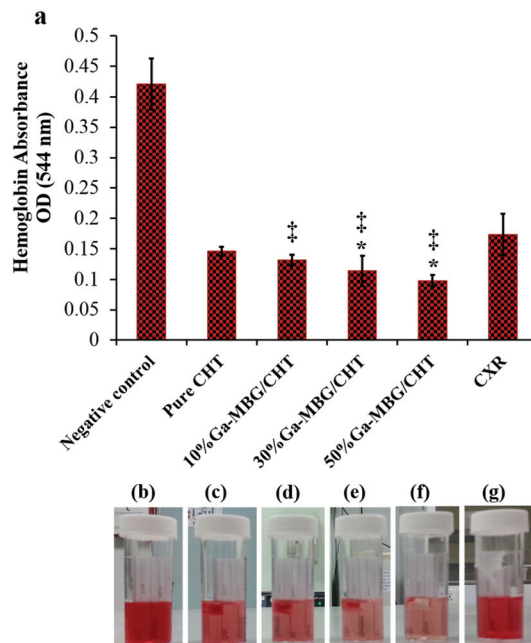

Fig. 8 (a) Influence of different Ga-MBG concentrations on blood clotting rates of CHT, as measured by the absorbance of hemoglobin released from uncoagulated RBCs. (b–g) Photographs showing less hemoglobin leaked from 30% Ga-MBG/CHT and 50% Ga-MBG/CHT than that of other samples. *$p < 0.05$ compared to CHT and ‡$p < 0.05$ compared to CXR. Reprinted with permission from ref. 77. Copyright 2017, American Chemical Society.

MS, Hou et al.[94] have recently prepared composites of MS and mesoporous zinc–calcium silicate (m-ZCS/MS) and investigated the influence of m-ZCS inclusion ranging from 5 to 15 wt% on the hemostatic response, antibacterial efficacy, and biocompatibility of MS. They found that the incorporation of 15 wt% m-ZCS into the MS matrix resulted in higher water absorption, degradability and enhanced L929 cells viability up to 5 days when compared with pure MS without m-ZCS. The study also suggested that m-ZCS/MS composites are very useful candidates for controlling bleeding and infections at the wounded area as the composites were able to accelerate hemostasis both in vitro and in vivo and exert an efficient antibacterial effect against E. coli. In a dose of 4 mg, inclusion of 15 wt% m-ZCS into the MS matrix remarkably reduced APTT and PT in vitro from 21s and 13s in MS to 13s and 7s, respectively. The MS with 15 wt% m-ZCS was also found to be superior over MS and the rest of the scaffolds at controlling hemorrhage in femoral arterial and liver injuries.[94]

7. Other mesoporous material-based hemostats

Li et al.[95] suggested that incorporation of 4 wt% curcumin-loaded mesoporous silica nanoparticles (CCM-MSNs) into polyvinyl pyrrolidone (PVP) nanofiber mats using electrospinning can improve the biological functions of the hybrid nanofibers (i.e. hemostatic properties, antibacterial effects and biocompat-

ibility). According to the results, the CCM-MSNs@PVP nanofibers (300%) with higher blood absorption ratios than that of the common hemostatic gauze (150%) facilitated hemostasis by promoting blood clot formation. The APTT and PT results also demonstrated that the nanofibers have the capability to activate both intrinsic and extrinsic pathways as APTT and PT were reduced on increasing the amount of hybrid nanofibers with respect to that of the control (blood free samples).[95] The *in vivo* results further revealed that the hybrid nanofibers can accelerate hemostasis in the liver injury model through absorption of the blood in the bleeding site and the formation of the hemostatic hydrogel, which in turn can activate the blood clotting system to staunch the wound bleeding. The results also confirmed that loading of CCM into MSNs not only endows nanofibers with efficient *in vitro* antibacterial characteristics against *methicillin-resistant Staphylococcus aureus* (MRSA), but also provided a good antimicrobial effect *in vivo* so that no infection was found in the wounded area. The composite nanofibers were also found to be biocompatible hemostatic materials as they showed no obvious toxic effect on the L929 cell viability.[95]

In a recent study by Wang *et al.*,[96] the effect of modified SBA-15 coating on the hemostatic performance and antibacterial efficacy of cotton fabrics was evaluated. The SBA-15 was modified with antibacterial polymeric *N*-halamine precursor (PSPH) and was then coated on cotton by a flat-screen printing technique (SBA-15-PSPH). To further enhance the antimicrobial efficacy of the cottons, they were also treated with 10% sodium hypochlorite solution (0.5% NaClO at pH 7, SBA-15-PSPH-Cl), a diluted household bleach.[96] The results revealed that cotton/SBA-15, cotton/SBA-15-PSPH and cotton/SBA-15-PSPH-Cl all possess greater thrombogenic activity than that of cotton, attributed to the large surface area (600–700 m^2 g^{-1}) and pore size (5–7 nm) of SBA-15 that could absorb a large amount of water from blood, concentrating clotting factors and promoting blood clotting. Among the tested samples, the SBA-15-PSPH-Cl exhibited superior bacterial killing effect against *S. aureus* (100%) and *E. coli* (99.99%), which was correlated to halogen exchange reactions between *N*-halamines and microorganisms, leading to destruction of the cell membrane of bacteria and death of the microorganism. Studies relating to SMMs and MBGs/polysaccharides hemostats and other mesoporous material-based hemostats are presented in Table 2.

8. Challenges and future prospects

The application of hemostatic agents after traumatic injury is of extreme importance, as uncontrolled bleeding is still the major cause of death in medical trauma, traffic accidents and the military.[97,98] However, despite the development of various hemostatic agents for clinical applications, current hemostats are still far behind the growing demand for medical care. In the present review, after summarizing the hemostasis process and preparation methods of both SMMs and MBGs, we highlighted the recent research advances in their *in vitro* and *in vivo* hemostatic activity. These mesoporous-based hemostats in different forms,

including particles, spheres, and composites, are found to hold great promise for hemostatic applications as they offer a suite of features that are important for achieving efficient hemostasis and preventing infections. The materials possess a well-defined mesoporous structure and high textural properties (*i.e.* high surface area and pore volume), endowing them with a higher water capacity compared to zeolites and clays, which is an extremely important parameter for the acceleration of blood clot formation. The materials can be doped with small quantities of trace elements, which can potentiate their hemostatic and/or antibacterial effect. Considering all the superior efficiencies of the mesoporous silica-based hemostats over the commercial inorganic hemostats (*i.e.* zeolites and clays), however, there exist gaps that need to be still filled.

Very little is known about the specific mechanisms of action of the SMMs and MBGs in the hemostasis process and more research both *in vitro* and *in vivo* should be performed in this direction. According to the recent reports proposing the MBGs for hemostatic application, their main focus was on formulations previously applied to bone tissue engineering applications and only a few therapeutic elements (*i.e.* Ga^{3+}, Zn^{2+} and Ag^+) have been assessed for their potential for hemostatic and antibacterial functions. For future research on this new generation of inorganic hemostatic materials, other biologically stimulating ions that accelerate hemostasis and prevent or treat bacterial infections need to be investigated. Similar to the conventional bioglasses, the MBGs are known to promote nucleation of HA on their surfaces during dissolution, as their composition is containing P. While there is a report concerning the antihemorrhagic effect of HA,[99] research studies undertaken so far have not evaluated the role of newly formed HA in the hemostasis process, so understanding the effect of HA formation on the coagulation process and the hemostatic ability of MBG-based materials is therefore a prerequisite. Similar to zeolite-based hemostats (*i.e.* QuikClot™), the application of powdery SMMs and MBGs may also raise some concerns as follows: (i) the low density and poor flowability of the materials in powder form make them unable to be immersed quickly in blood; (ii) using powdery SMMs and MBGs on an active bleeding site may lead to dust pollution deteriorating the operating environment. (iii) The powders can be flushed out or blown away by rapid bleeding from high-flow blood vessels if not compressed with a gauze on the top of powder.[60] (iv) The difficulty in removing the powders from the bleeding site that can easily form thick callus in contact with blood is an additional concern leading to patients experiencing more pain. (v) The application of powdery hemostats can also lead to local damage owing to foreign body reactions and systemic embolization.[100] These are the reasons why loose powder forms of previously developed commercial zeolite-based hemostats (*i.e.* QuikClot™) fell out of favor and the next generation of inorganic clays (*i.e.* kaolin) has been attached and coated on the gauze (QuikClot Combat Gauze™). However, as explained earlier, this generation of hemostats often failed to achieve rapid hemostasis.[6] Although granulation of the mesoporous materials can dispel the shortcomings of the powdery materials, there could be additional

Table 2 Studies relating to SMM- and MBG-based hemostatic composites

Ref.	SMM- and MBG-based hemostatic composites	Blood clotting rate as measured by the absorbance of hemoglobin and/or BCI	APTT and PT		In vivo model/blood loss (mL)/time to hemostasis	Remarks
			APTT (s)	PT (s)	Rabbit model of lethal extremity arterial bleeding	- CSSX samples significantly shortened the APTT values compared with negative control
88	CSSX-0		−21	−12		- CSSX-25 was superior over the other tested samples as it decreased both the time to hemostasis and the blood loss volume
	CSSX-20		20	11		
	CSSX-25		18	14		
	CSSX-55		21	13		
	Negative control		32	13		
					Blood loss (mL)	
	CSSX-0	—			21.6	
	CSSX-20				16.7	
	CSSX-25				15.9	
	CSSX-55				19.4	
					Time to hemostasis (s)	
	CSSX-0				141.0	
	CSSX-20				128.2	
	CSSX-25				95.5	
	CSSX-55				145.9	
		Hemoglobin absorbance OD (544 nm)				
89	Pure CHT	0.14				Incorporation of higher concentration of 1% Ga-MBG in CHT matrix resulted in lower absorbance value of the hemoglobin solution than other scaffolds and CXR, confirming a higher clotting rate
	10% Ga-MBG/CHT	0.13				
	30% Ga-MBG/CHT	0.11				
	50% Ga-MBG/CHT	0.09				
	CXR	0.17				
	Negative control	0.42				
			At a concentration of 2 mg:			
94	MS	—	22.9	7612.3	Rabbit ear vein and back injuries, femoral artery and liver injuries	The MS with higher mZSC content (15 wt%) was found more efficient product since not only decreased both APTT and PT compared to MS, but also reduced remarkably hemostatic time in rabbit models of ear vein, skin, arterial and liver injuries
	5mZSC		17.4	−10		
	10mZSC		−15	−9		
	15mZSC		12.8	7		
			At a concentration of 4 mg:		Time to hemostasis (s)	
	MS		−22	12.3	76	
	5mZSC		−16	−9.8	−61	
	10mZSC		−13	−8	−55	
	15mZSC		−12	7	52	
					Rabbit back injury	
	MS				69	
	5mZSC				−56	
	10mZSC				−50	
	15mZSC				46	
					Rabbit femoral artery injury	
	MS				155	
	5mZSC				−142	
	10mZSC				−130	
	15mZSC				122	
					Rabbit liver injury	
	MS				132	
	5mZSC				122	
	10mZSC				114	
	15mZSC				102	

Table 2 (Contd.)

Ref.	SMM- and MBG-based hemostatic composites	Blood clotting rate as measured by the absorbance of hemoglobin and/or BCI	APTT and PT	*In vivo* model/blood loss (mL)/time to hemostasis	Remarks
96	Cotton	BCI (s) −75			All the samples demonstrated lower BCI values than cotton, particularly cotton/SBA-15, representing the high thrombogenic activity of SBA-15
	Cotton/SBA-15	−56			
	Cotton/SBA-15-PSPH	−60			
	Cotton/SBA-15-PSPH-Cl	−63			

concern about the granular nature of the materials as they may lead to inflammatory granuloma formation similar to that of QuikClot™.[6] Therefore, anchoring MBG and/or SMM particles into a template (*i.e.* gauze or foam) which has inherent hemostatic efficacy can be one strategy to tackle these issues. This technology can further potentiate the hemostatic effect of MBGs and/or SMMs, holding it firmly over the injured site until bleeding stops. While a few studies have evaluated the hemostatic effect of the new inorganic hemostats when they were incorporated into the supports,[89,96] more studies need to be conducted to ascertain their efficacy even when incorporated and/or impregnated into a template. Additionally, since there are contradictory findings concerning the biocompatibility of the SMMs,[101–105] a careful evaluation of cell response to SMMs will therefore be necessary to gain a clear understanding of the cytocompatibility of the SMMs.

In conclusion, with a further understanding of their corresponding hemostatic mechanisms in large animal models *in vivo*, it is expected that these mesoporous-based hemostats may be promising candidates for improving the quality of life for both civilian and military trauma patients who suffer from uncontrolled bleeding and infection.

Conflicts of interest

There are no conflicts to declare.

Acknowledgements

References

1 H. R. Champion, R. F. Bellamy, C. P. Roberts and A. Leppaniemi, *J. Trauma Acute Care Surg.*, 2003, **54**, S13–S19.

2 J. B. Holcomb, N. R. McMullin, L. Pearse, J. Caruso, C. E. Wade, L. Oetjen-Gerdes, H. R. Champion, M. Lawnick, W. Farr and S. Rodriguez, *Ann. Surg.*, 2007, **245**, 986.

3 J. B. Holcomb, *J. Trauma Acute Care Surg.*, 2005, **58**, 1298–1303.

4 H. B. Alam, D. Burris, J. A. DaCorta and P. Rhee, *Mil. Med.*, 2005, **170**, 63–69.

5 D. S. Kauvar, R. Lefering and C. E. Wade, *J. Trauma Acute Care Surg.*, 2006, **60**, S3–S11.

6 S. Pourshahrestani, E. Zeimaran, I. Djordjevic, N. A. Kadri and M. R. Towler, *Mater. Sci. Eng., C*, 2016, **58**, 1255–1268.

7 J. Granville-Chapman, N. Jacobs and M. Midwinter, *Injury*, 2011, **42**, 447–459.

8 H. E. Achneck, B. Sileshi, R. M. Jamiolkowski, D. M. Albala, M. L. Shapiro and J. H. Lawson, *Ann. Surg.*, 2010, **251**, 217–228.

9 S. Butenas and K. Mann, *Biochemistry*, 2002, **67**, 3–12.

10 G. Casey, *Nurs. Stand.*, 2003, **18**, 45–51.

11 K. Broos, H. B. Feys, S. F. De Meyer, K. Vanhoorelbeke and H. Deckmyn, *Blood Rev.*, 2011, **25**, 155–167.

12 J. H. Morrissey, *Thromb. Haemostasis*, 2001, **86**, 66–74.

13 M. B. Gorbet and M. V. Sefton, *Biomaterials*, 2004, **25**, 5681–5703.

14 N. Mackman, R. E. Tilley and N. S. Key, *Arterioscler., Thromb., Vasc. Biol.*, 2007, **27**, 1687–1693.

15 J. Rouquerol, D. Avnir, C. Fairbridge, D. Everett, J. Haynes, N. Pernicone, J. Ramsay, K. Sing and K. Unger, *Pure Appl. Chem.*, 1994, **66**, 1739–1758.

16 N. Rahmat, A. Z. Abdullah and A. R. Mohamed, *Am. J. Appl. Sci.*, 2010, **7**, 1579.

17 G. Gonzalez, A. Sagarzazu and T. Zoltan, *J. Drug Delivery*, 2013, **2013**, 803585.

18 M. Manzano and M. Vallet-Regí, *J. Mater. Chem.*, 2010, **20**, 5593–5604.

19 C. Kresge, M. Leonowicz, W. Roth, J. Vartuli and J. Beck, *Nature*, 1992, **359**, 710–712.

20 G. S. Attard, J. C. Glyde and C. G. Göltner, *Nature*, 1995, **378**, 366.

21 A. Monnier, F. Schüth, Q. Huo, D. Kumar, D. Margolese, R. Maxwell, G. Stucky, M. Krishnamurty, P. Petroff and A. Firouzi, *Science*, 1993, **261**, 1299–1303.

22 J. Vartuli, C. Kresge, M. Leonowicz, A. Chu, S. McCullen, I. Johnson and E. Sheppard, *Chem. Mater.*, 1994, **6**, 2070–2077.

23 M. Vallet-Regí, M. M. Garcia and M. Colilla, *Biomedical applications of mesoporous ceramics: drug delivery, smart materials and bone tissue engineering*, CRC Press, 2012.

24 I. Izquierdo-Barba and M. Vallet-Regí, *Biomed. Glasses*, 2015, **1**, 140–150.

25 M. Vallet-Regí, F. Balas and D. Arcos, *Angew. Chem., Int. Ed.*, 2007, **46**, 7548–7558.

26 I. I. Slowing, B. G. Trewyn, S. Giri and V. Y. Lin, *Adv. Funct. Mater.*, 2007, **17**, 1225–1236.

27 A. Baeza, M. Colilla and M. Vallet-Regí, *Expert Opin. Drug Delivery*, 2015, **12**, 319–337.

28 Y. Song, Y. Li, Q. Xu and Z. Liu, *Int. J. Nanomed.*, 2017, **12**, 87.

29 N. Gargiulo, I. Attianese, G. G. Buonocore, D. Caputo, M. Lavorgna, G. Mensitieri and M. Lavorgna, *Microporous Mesoporous Mater.*, 2013, **167**, 10–15.

30 M. Stanzione, N. Gargiulo, D. Caputo, B. Liguori, P. Cerruti, E. Amendola, M. Lavorgna and G. Buonocore, *Eur. Polym. J.*, 2017, **89**, 88–100.

31 E. Zúñiga, L. Belmar, L. Toledo, C. Torres, B. L. Rivas, S. A. Sánchez and B. F. Urbano, *Eur. Polym. J.*, 2017, **95**, 358–367.

32 I. Izquierdo-Barba, M. Colilla and M. Vallet-Regí, *J. Nanomater.*, 2008, **2008**, 60.

33 X. Yan, C. Yu, X. Zhou, J. Tang and D. Zhao, *Angew. Chem., Int. Ed.*, 2004, **43**, 5980–5984.

34 X. Yan, C. Yu, X. Zhou, J. Tang and D. Zhao, *Angew. Chem., Int. Ed.*, 2004, **43**, 5980–5984.

35 P. Jiang, F. Qu, H. Lin, X. Wu, R. Xing and J. Zhang, *IET Nanobiotechnol.*, 2012, **6**, 93–101.

36 C. J. Brinker, Y. Lu, A. Sellinger and H. Fan, *Adv. Mater.*, 1999, **11**, 579–585.

37 I. Izquierdo-Barba, A. J. Salinas and M. Vallet-Regí, *Int. J. Appl. Glass Sci.*, 2013, **4**, 149–161.

38 M. Vallet-Regí, I. Izquierdo-Barba and M. Colilla, *Philos. Trans. R. Soc., A*, 2012, **370**, 1400–1421.

39 Y. Zhou, M. Shi, J. R. Jones, Z. Chen, J. Chang, C. Wu and Y. Xiao, *Int. Mater. Rev.*, 2017, 1–23.

40 X. Zhang, D. Zeng, N. Li, J. Wen, X. Jiang, C. Liu and Y. Li, *Sci. Rep.*, 2016, **6**, 19361.

41 A. Philippart, N. Gómez-Cerezo, D. Arcos, A. J. Salinas, E. Boccardi, M. Vallet-Regi and A. R. Boccaccini, *J. Non-Cryst. Solids*, 2017, **455**, 90–97.

42 M. Alcaide, P. Portoles, A. López-Noriega, D. Arcos, M. Vallet-Regí and M. Portoles, *Acta Biomater.*, 2010, **6**, 892–899.

43 N. Gargiulo, A. M. Cusano, F. Causa, D. Caputo and P. A. Netti, *J. Mater. Sci. Mater. Med.*, 2013, **24**, 2129–2135.

44 A. Bari, N. Bloise, S. Fiorilli, G. Novajra, M. Vallet-Regí, G. Bruni, A. Torres-Pardo, J. M. González-Calbet, L. Visai and C. Vitale-Brovarone, *Acta Biomater.*, 2017, **55**, 493–504.

45 Y. Li, Y.-Z. Liu, T. Long, X.-B. Yu, T. T. Tang, K.-R. Dai, B. Tian, Y.-P. Guo and Z.-A. Zhu, *J. Mater. Sci. Mater. Med.*, 2013, **24**, 1951–1961.

46 X. Wang and W. Li, *Nanotechnology*, 2016, **27**, 225102.

47 X. Wang, Y. Zhang, Y. Ma, D. Chen, H. Yang and M. Li, *Ceram. Int.*, 2016, **42**, 3609–3617.

48 C. Wu and J. Chang, *Interface Focus*, 2012, **2**, 292–306.

49 L. Polo, N. Gómez-Cerezo, E. Aznar, J.-L. Vivancos, F. Sancenon, D. Arcos, M. Vallet-Regi and R. Martinez-Manez, *Acta Biomater.*, 2017, **50**, 114–126.

50 T. A. Ostomel, Q. Shi and G. D. Stucky, *J. Am. Chem. Soc.*, 2006, **128**, 8384–8385.

51 M. Mikaelsson, in *Coagulation and blood transfusion*, Springer, 1991, pp. 29–37.

52 S. R. Coughlin, *Nature*, 2000, **407**, 258–264.

53 T. Halkier, *Mechanisms in blood coagulation, fibrinolysis and the complement system*, Cambridge University Press, 1991.

54 M. Hoffman, *J. Thromb. Thrombolysis*, 2003, **16**, 17–20.

55 T. A. Ostomel, Q. Shi, C. K. Tsung, H. Liang and G. D. Stucky, *Small*, 2006, **2**, 1261–1265.

56 X. Wu, J. Wei, X. Lu, Y. Lv, F. Chen, Y. Zhang and C. Liu, *Biomed. Mater.*, 2010, **5**, 035006.

57 S. E. Baker, A. M. Sawvel, J. Fan, Q. Shi, N. Strandwitz and G. D. Stucky, *Langmuir*, 2008, **24**, 14254–14260.

58 Y. Li, A. M. Sawvel, Y.-S. Jun, S. Nownes, M. Ni, D. Kudela, G. D. Stucky and D. Zink, *Toxicol. Res.*, 2013, **2**, 136–144.

59 Z. Chen, F. Li, C. Liu, J. Guan, X. Hu, G. Du, X. Yao, J. Wu and F. Tian, *J. Mater. Chem. B*, 2016, **4**, 7146–7154.

60 H. Hong, C. Wang, Y. Yuan, X. Qu, J. Wei, Z. Lin, H. Zhou and C. Liu, *RSC Adv.*, 2016, **6**, 78930–78935.

61 J. S. Boateng, K. H. Matthews, H. N. Stevens and G. M. Eccleston, *J. Pharm. Sci.*, 2008, **97**, 2892–2923.

62 J. G. Penn-Barwell, K. V. Brown and C. A. Fries, *Curr. Rev. Musculoskelet. Med.*, 2015, **8**, 312–317.

63 J. Blaker, S. Nazhat and A. Boccaccini, *Biomaterials*, 2004, **25**, 1319–1329.

64 A. Balamurugan, G. Balossier, D. Laurent-Maquin, S. Pina, A. Rebelo, J. Faure and J. Ferreira, *Dent. Mater.*, 2008, **24**, 1343–1351.

65 M. Bellantone, H. D. Williams and L. L. Hench, *Antimicrob. Agents Chemother.*, 2002, **46**, 1940–1945.

66 D. Parsons, P. Bowler, V. Myles and S. Jones, *Wounds*, 2005, **17**, 222–232.

67 Y. Matsumura, K. Yoshikata, S.-I. Kunisaki and T. Tsuchido, *Appl. Environ. Microbiol.*, 2003, **69**, 4278–4281.

68 S. Liau, D. Read, W. Pugh, J. Furr and A. Russell, *Lett. Appl. Microbiol.*, 1997, **25**, 279–283.

69 A. Russell, F. Path, F. P. Sl and W. Hugo, *Prog. Med. Chem.*, 1994, **31**, 351.

70 R. Belly and G. Kydd, *Dev. Ind. Microbiol.*, 1982, **23**, 567–578.

71 S. Thomas, *World Wide Wounds*, 2004.

72 C. Dai, Y. Yuan, C. Liu, J. Wei, H. Hong, X. Li and X. Pan, *Biomaterials*, 2009, **30**, 5364–5375.

73 G. Hu, L. Xiao, P. Tong, D. Bi, H. Wang, H. Ma, G. Zhu and H. Liu, *Int. J. Nanomed.*, 2012, **7**, 2613.

74 S. P. Valappil, D. Ready, E. A. A. Neel, D. M. Pickup, W. Chrzanowski, L. A. O'Dell, R. J. Newport, M. E. Smith, M. Wilson and J. C. Knowles, *Adv. Funct. Mater.*, 2008, **18**, 732–741.

75 C. Chitambar and J. Narasimhan, *Pathobiology*, 1991, **59**, 3–10.

76   S. Pourshahrestani, E. Zeimaran, N. A. Kadri, N. Gargiulo, S. Samuel, S. V. Naveen, T. Kamarul and M. R. Towler, *J. Mater. Chem. B*, 2016, **4**, 71–86.

77   S. Pourshahrestani, N. A. Kadri, E. Zeimaran, N. Gargiulo, S. Samuel, S. V. Naveen, K. Hasikin, T. Kamarul and M. R. Towler, *Biomed. Mater.*, 2018, **13**, 025020.

78   G. Hu, L. Xiao, P. Tong, D. Bi, H. Wang, H. Ma, G. Zhu and H. Liu, *Int. J. Nanomed.*, 2012, **7**, 2613.

79   X. Yang, W. Liu, N. Li, M. Wang, B. Liang, I. Ullah, A. L. Neve, Y. Feng, H. Chen and C. Shi, *Biomater. Sci.*, 2017, **5**, 2357–2368.

80   S.-Y. Ong, J. Wu, S. M. Moochhala, M.-H. Tan and J. Lu, *Biomaterials*, 2008, **29**, 4323–4332.

81   G. Lan, B. Lu, T. Wang, L. Wang, J. Chen, K. Yu, J. Liu, F. Dai and D. Wu, *Colloids Surf., B*, 2015, **136**, 1026–1034.

82   Y. Wang, Y. Fu, J. Li, Y. Mu, X. Zhang, K. Zhang, M. Liang, C. Feng and X. Chen, *Carbohydr. Polym.*, 2018, **200**, 6–14.

83   M. Shin, S.-G. Park, B.-C. Oh, K. Kim, S. Jo, M. S. Lee, S. S. Oh, S.-H. Hong, E.-C. Shin and K.-S. Kim, *Nat. Mater.*, 2017, **16**, 147.

84   H. Mirzadeh, N. Yaghobi, S. Amanpour, H. Ahmadi, M. A. Mohagheghi and F. Hormozi, *Iran. Polym. J.*, 2002, **11**, 63–68.

85   S. B. Rao and C. P. Sharma, *J. Biomed. Mater. Res.*, 1997, **34**, 21–28.

86   J. Yang, F. Tian, Z. Wang, Q. Wang, Y. J. Zeng and S. Q. Chen, *J. Biomed. Mater. Res., Part B*, 2008, **84**, 131–137.

87   L. B. Williams and S. E. Haydel, *Int. Geol. Rev.*, 2010, **52**, 745–770.

88   C. Dai, C. Liu, J. Wei, H. Hong and Q. Zhao, *Biomaterials*, 2010, **31**, 7620–7630.

89   S. Pourshahrestani, E. Zeimaran, N. A. Kadri, N. Gargiulo, H. M. Jindal, S. V. Naveen, S. D. Sekaran, T. Kamarul and M. R. Towler, *ACS Appl. Mater. Interfaces*, 2017, **9**, 31381–31392.

90   S. Pourshahrestani, E. Zeimaran, N. A. Kadri, N. Gargiulo, H. M. Jindal, S. V. Naveen, S. D. Sekaran, T. Kamarul and M. R. Towler, *ACS Appl. Mater. Interfaces*, 2017, **9**, 31381–31392.

91   J. L. Antisdel, J. L. West-Denning and R. Sindwani, *Otolaryngol. – Head Neck Surg.*, 2009, **141**, 353–357.

92   M. d. L. P. Biondo-Simões, R. Petrauskas, A. G. Dobrowolski, G. Godoy, F. Kaiber and S. O. Ioshii, *Acta Cir. Bras.*, 2007, **22**, 29–33.

93   K. Björses and J. Holst, *Eur. J. Vasc. Endovasc. Surg.*, 2007, **33**, 363–370.

94   Y. Hou, Y. Xia, Y. Pan, S. Tang, X. Sun, Y. Xie, H. Guo and J. Wei, *Mater. Sci. Eng., C*, 2017, **76**, 340–349.

95   D. Li, W. Nie, L. Chen, Y. Miao, X. Zhang, F. Chen, B. Yu, R. Ao, B. Yu and C. He, *RSC Adv.*, 2017, **7**, 7973–7982.

96   Y. Wang, M. Yin, Z. Li, Y. Liu, X. Ren and T.-S. Huang, *Colloids Surf., B*, 2018, **165**, 199–206.

97   A. M. Behrens, M. J. Sikorski and P. Kofinas, *J. Biomed. Mater. Res., Part A*, 2014, **102**, 4182–4194.

98   H. B. Alam, E. Koustova and P. Rhee, *World J. Surg.*, 2005, **29**, S7–S11.

99   T. A. Ostomel, Q. Shi, P. K. Stoimenov and G. D. Stucky, *Langmuir*, 2007, **23**, 11233–11238.

100 M. Bustamante-Balén and G. Plumé, *World J. Gastrointest. Pathophysiol.*, 2014, **5**, 284.

101 S. Al-Salam, G. Balhaj, S. Al-Hammadi, M. Sudhadevi, S. Tariq, A. V. Biradar, T. Asefa and A.-K. Souid, *Toxicol. Sci.*, 2011, **122**, 86–99.

102 M. T. Al Samri, A. V. Biradar, A. R. Alsuwaidi, G. Balhaj, S. Al-Hammadi, S. Shehab, S. Al-Salam, S. Tariq, T. Pramathan and S. Benedict, *Int. J. Nanomed.*, 2012, **7**, 3111.

103 E. H. Aburawi, M. A. Qureshi, D. Oz, P. Jayaprakash, S. Tariq, R. S. Hameed, S. Das, A. Goswami, A. V. Biradar and T. Asefa, *Chem. Res. Toxicol.*, 2012, **26**, 26–36.

104 S. P. Hudson, R. F. Padera, R. Langer and D. S. Kohane, *Biomaterials*, 2008, **29**, 4045–4055.

105 T. Heikkilä, H. A. Santos, N. Kumar, D. Y. Murzin, J. Salonen, T. Laaksonen, L. Peltonen, J. Hirvonen and V.-P. Lehto, *Eur. J. Pharm. Biopharm.*, 2010, **74**, 483–494.